CrystEngComm

PAPER

View Article Online
View Journal | View Issue

Cite this: *CrystEngComm*, 2025, **27**, 1128

Aqueous solution as a playground of $\{MoO_4\}$, $\{Mo_4O_{12}\}$, $\{Mo_8O_{26}\}$, $\{Mo_8V_5O_{40}\}$ and $\{V_7Mo_2O_{27}\}$ species in the presence of carboxylic acids and $[Co(C_2O_4)(NH_3)_4]^+$ or $[Co(en)_3]^{3+}$ cations†

D. Kuzman,*[a] V. Damjanović,[b] M. Cindrić *[a] and V. Vrdoljak[a]

Received 26th November 2024,
Accepted 9th January 2025

DOI: 10.1039/d4ce01187b

rsc.li/crystengcomm

Nine tetraammineoxalatocobalt(III) salts built of different oxomolybdate anions, *i.e.* $\{\beta\text{-}Mo_8O_{26}\}^{4-}$ (in **1**, **2**, and **6**), $\{Na_2Mo_8O_{29}(H_2O)_4\}_n^{4m-}$ (in **3**), $\{[\beta\text{-}Mo_8O_{26}(H_2O)_2][\gamma\text{-}Mo_8O_{26}]\}^{8-}$ (in **4**), $\{\gamma\text{-}Mo_8O_{26}(H_2O)_2\}^{4-}$ (in **5**, **7**), $\{Mo_4O_{12}(C_4H_4O_4)\}_n^{4m-}$ (in **8**), and $\{\gamma\text{-}Mo_8O_{26}\}_n^{4m-}$ (in **9**) were isolated as the product(s) of the reaction of sodium molybdate and $[Co(C_2O_4)(NH_3)_4]NO_3{\cdot}H_2O$ in the presence of acetic or succinic acid. Octamolybdate isomers, namely distinct β- and γ-octamolybdates along with complex cobalt(III) cations and water molecules are the building blocks of three-dimensional supramolecular frameworks (in **1**, **2**, and **4**–**7**). In some cases, octamolybdate subunits are interconnected by sodium cations or a pair of shared oxygen atoms to form infinite anionic chains (in **3** and **9**), or by coordinated succinate anions to assemble into a two-dimensional MOF (in **8**). When $[Co(CO_3)(NH_3)_4]NO_3{\cdot}H_2O$ was used as a precursor, neutral compounds $[Mo_5Co_2O_{17}(HCO_3)(H_4C_4O_4H)(NH_3)_7]$ (**10**) and $[Mo_7Co_2O_{18}(NH_3)_7]$ (**11**) were obtained. Furthermore, two molybdovanadates of proposed formula $[Co(C_2O_4)(NH_3)_4]_2[H_2Mo_8V_5O_{40}Na_2(H_2O)_8]$ (**12**) and unique $Na_3[Co(en)_3][V_7Mo_2O_{27}]$ (**13**) were obtained in the reactions of sodium molybdate, ammonium vanadate and $[Co(C_2O_4)(NH_3)_4]NO_3{\cdot}H_2O$ or $[Co(en)_3]Cl_3$ in the presence of acetic or succinic acid, respectively. The products **1**–**9** were characterized in the solid state *via* single-crystal X-ray diffraction, infrared spectroscopy, and thermogravimetric and elemental analyses.

Introduction

Polyoxomolybdates represent compounds of highly versatile structures and have potential applications as functional materials in many scientific fields.[1–3] The great majority of polyoxomolybdates are discrete molecules, generated *via* condensation of molybdate anions, MoO_4^{2-}. However, sometimes the condensation process may continue yielding infinite molecular self-assemblies organized in 1D chains, 2D layers or 3D networks. The design of polyoxomolybdate architectures is non-trivial because their formation is highly dependent on the reaction conditions. Although the pH of the reaction mixture and temperature are considered the most important factors affecting speciation, other parameters such as nature of the used counter ion, ionic strength of the solution or the presence of chelating or reducing agents must also be considered. The ability to control the aggregation process or linkage of the building blocks to pre-establish structure-type as well as engineer the physical properties is an immeasurable challenge.[4] One-pot synthesis is a common method used for the preparation of most polyoxomolybdates but despite its apparent simplicity, the above-mentioned conditions under which synthesis is performed act as crucial structure defining parameters. A slight change in one of these parameters can lead to a completely different polyoxomolybdate architecture that prevents the ability for reliable control or design of the framework. Polyoxomolybdates are generally anionic and associated with charge-balancing cations, such as alkali or alkaline earth cations. These cations play a crucial role in controlling the dissolution, precipitation, and purification of POMs. More complex cations, such as $[ML_n]^{x+}$ (where M is a d or an f block element; L is a mono or polydentate ligand), exhibit various interaction modes, including hydrogen bonding, ion–dipole

[a] *Department of Chemistry, University of Zagreb Faculty of Science, Horvatovac 102a, Zagreb, Croatia. E-mail: marina.chem@pmf.hr*
[b] *Department of Chemistry and Biochemistry, University of Zagreb School of Medicine, Šalata 3, Zagreb, Croatia*

† Electronic supplementary information (ESI) available: (1) Additional experimental data, (2) thermogravimetric data, (3) IR data, (4) analytical data, (5) crystallographic data, (6) tables of selected bond distances and angles and of hydrogen bond parameters, (7) TGA curves, and (8) NMR spectra. Crystallographic data sets for the structures **3**–**9** are available through the Cambridge Structural Database with deposition numbers CCDC 2404581–2404587. For ESI and crystallographic data in CIF or other electronic format see DOI: https://doi.org/10.1039/d4ce01187b

interactions, partial covalency, and van-der-Waals interactions.[5,6] These divergent interaction modes facilitate templating and stabilization from both within and outside the POMs, contribute to framework construction and supramolecular assembly, and enhance reactivity and speciation.[7] The unique structure-directing properties of different organic, inorganic or inorganic–organic cations have been exploited to design new organic–inorganic hybrid materials using octamolybdate isomers as versatile building blocks.[8–10] So far, eight isomers of octamolybdates are known: α, β, γ, δ, ε, ζ, η and θ,[11] with the α- and β-isomers being the best-known and frequently encountered.[12] In order to explain the inter-conversion of α- and β-forms, Xi and Ozawa[13] proposed the γ-isomer as an intermediate in the isomerization process between these two forms. The α-isomer is built up from a ring of six MoO_6 edge-shared octahedra bicapped by MoO_4 tetrahedra,[14] β-$[Mo_8O_{26}]^{4-}$ consists of three distinct types of edge-shared MoO_6 groups[15] unlike the γ-isomer[7,16] which is built from six MoO_6 octahedra and two MoO_5 square pyramid subunits.

The various structural isomers of octamolybdates are present and play a significant role in developing many organic–inorganic hybrid materials, which are of great interest in the field. For instance, the δ-isomer can be found in the compounds $[(\eta\text{-}C_5Me_5Rh)_2(\mu\text{-}SMe)_3]_4[(Mo_8O_{26})]\cdot 2CH_3CN$ and $[\{Cu(4,4'\text{-bipy})\}_4Mo_8O_{26}]$. The ε-isomer is present in the compound $[\{Ni(H_2O)_2(4,4'\text{-bipy})_2\}_2Mo_8O_{26}]$, while the ξ-isomer is present in the compound $[\{M(phen)_2\}(\xi\text{-}Mo_8O_{26})]$, where M can be either Ni or Co and phen refers to 1,10-phenantroline. Such isomeric forms of octamolybdates serve as versatile structural blocks, facilitating the formation of organo–inorganic hybrid materials with tailored properties.[17]

As part of our efforts to systematize[18–20] the factors that direct the polyoxomolybdate composition, in this study we explored the influence of different Co(III) ammine complex cations, along with the pH value of reaction medium and the temperature at which the reaction is conducted. The selected cations exhibit varying stability when dissolved in solution, which can impact how they interact with other species. Moreover, they can act as either donors or acceptors of hydrogen bonds. This ability influences reactions, affects solubility, and contributes to the formation of different hybrids.

Furthermore, the similarity in chemistry of polyoxomolybdates and polyoxovanadates[21] prompted us to investigate whether the addition of ammonium vanadate will influence the composition and structure of polyoxomolybdate. By applying solution-based methods we were able to isolate thirteen products of different nuclearity and composition (Scheme 1).

The structures of the seven compounds **3–9** are reported here for the first time. Compound **4** represents the first example of a salt containing both β- and γ-forms of octamolybdate anion in its structure.

Results and discussion

Synthesis

As a continuation of our previous research,[14–16] herein we have investigated reaction systems containing $[MoO_4]^{2-}$ anions, $[Co(C_2O_4)(NH_3)_4]^+$ or $[Co(CO_3)(NH_3)_4]^+$ cations, and acetic or succinic acid at different pH values or temperatures (Scheme 1, Table 1). The pH value of the reaction mixtures was between 2 and 5 (Tables S1–S5†). Depending on the acid concentration, along with the reaction temperature we were able to isolate ten crystalline products of different nuclearity. The crystal structures of compounds **1**, **2**, and **11** are described in the literature[14] but crystals were obtained under the different reaction conditions.

Solution based reactions between molybdate anions, tetraammineoxalatocobalt(III) cations and acid were performed in aqueous medium. When the reactions were

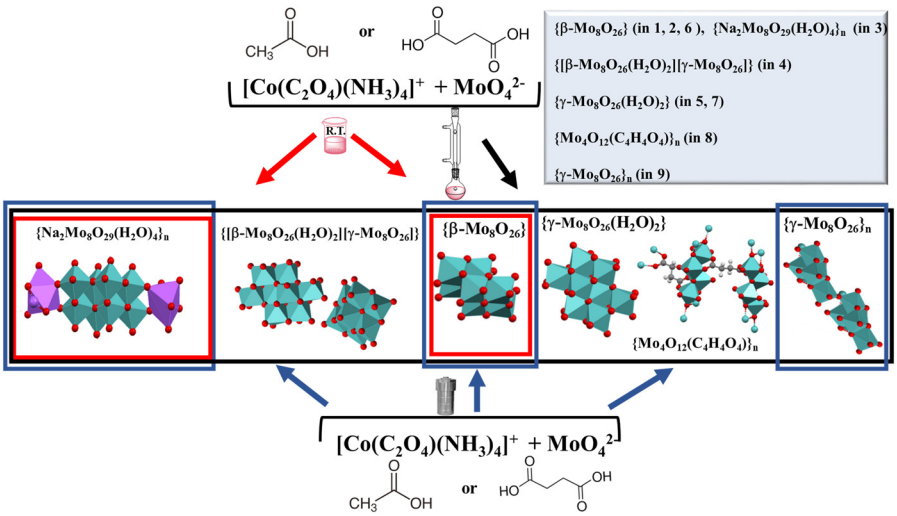

Scheme 1 Schematic representation of the diverse polyoxomolybdates formed utilizing solution-based synthesis methods.

Table 1 Overview of polyoxomolybdates **1–11** and the corresponding reaction conditions for their synthesis

	[Co][a] + MoO_4^{2-}					
	Acetic acid			Succinic acid		
Method	R.T.	Reflux	Hydrothermal 110 °C	R.T.	Reflux	Hydrothermal 110 °C
Compound	pH range			pH range		
$[Co(C_2O_4)(NH_3)_4]_4[\beta\text{-}Mo_8O_{26}]\cdot 12H_2O$ (**1**)	2.0–5.0	3.5–5.0	3.5–5.0	3.5	3.5–5.0	3.5–5.0
$[Co(C_2O_4)(NH_3)_4]_4[\beta\text{-}Mo_8O_{26}]\cdot 10H_2O$ (**2**)	2.0–5.0		3.5–5.0			
$[Co(C_2O_4)(NH_3)_4]_{4n}[Na_2Mo_8O_{29}(H_2O)_4]_n\cdot 6nH_2O$ (**3**)[b]		3.5–5.0		4.5	3.5–5.0	3.5–5.0
$[Co(C_2O_4)(NH_3)_4]_8[\beta\text{-}Mo_8O_{26}(H_2O)_2][\gamma\text{-}Mo_8O_{26}]\cdot 12H_2O$ (**4**)		>3.5	>3.5			
$[Co(C_2O_4)(NH_3)_4]_4[\gamma\text{-}Mo_8O_{26}(H_2O)_2]\cdot 6H_2O$ (**5**)		>3.5	>3.5			
$[Co(C_2O_4)(NH_3)_4]_4[\beta\text{-}Mo_8O_{26}]\cdot 4H_2O\cdot C_4H_6O_4$ (**6**)				2.0–3.5	2.5–5.0	3.5–5.0
$[Co(C_2O_4)(NH_3)_4]_4[\gamma\text{-}Mo_8O_{26}(H_2O)_2]\cdot 12H_2O$ (**7**)					3.5–5.0	3.5–5.0
$[Co(C_2O_4)(NH_3)_4]_{2n}[Mo_4O_{12}(H_4C_4O_4)]_n\cdot 3nH_2O$ (**8**)					3.5–5.0	3.5–5.0
$[Co(C_2O_4)(NH_3)_4]_{4n}[\gamma\text{-}Mo_8O_{26}]_n\cdot 9nH_2O$ (**9**)						2.0
$[Mo_5Co_2O_{17}(HCO_3)(C_4H_4O_4H)(NH_3)_7]\cdot 5H_2O$ (**10**)	3.0–4.0	3.0–4.0	3.0–4.0	3.0–4.0	3.0–4.0	3.0–4.0
$[Mo_5Co_2O_{18}(NH_3)_7]\cdot 5H_2O$ (**11**)	3.0–4.0	3.0–4.0	3.0–4.0	3.0–4.0	3.0–4.0	3.0–4.0

[a] Compounds **1–9** were obtained by the solution based methods using $[Co(C_2O_4)(NH_3)_4]NO_3\cdot H_2O$, while **10** and **11** were obtained using $[Co(CO_3)(NH_3)_4]NO_3$ as a [Co] precursor. [b] Compound **3** was also obtained by mechanochemical synthesis.

performed at room temperature with the addition of acetic acid, they resulted in the formation of a mixture of unstable dark pink rods of $[Co(C_2O_4)(NH_3)_4]_4[\beta\text{-}Mo_8O_{26}]\cdot 12H_2O$ (**1**) and stable pink plates of $[Co(C_2O_4)(NH_3)_4]_4[\beta\text{-}Mo_8O_{26}]\cdot 10H_2O$ (**2**), regardless of the applied pH value. In the reaction with succinic acid (pH around 4.5), a pink powder precipitated immediately after mixing the reactants, and its transformation into polymer $[Co(C_2O_4)(NH_3)_4]_{4n}[Na_2Mo_8O_{29}(H_2O)_4]_n\cdot 6nH_2O$ (**3**) was completed within four days. At higher concentration of succinic acid (pH around 3.5) pink powder transformation resulted in unstable dark pink rods of **1** after several days, while at lower pH values (pH range between 2.0 and 3.5), the final product of transformation was cocrystal $[Co(C_2O_4)(NH_3)_4]_4[\beta\text{-}Mo_8O_{26}]\cdot 4H_2O\cdot C_4H_6O_4$ (**6**).

When the reactions were carried out at higher temperatures in the presence of acetic acid, and within the pH range between 3.5 and 5.0, a mixture of pink plates of polymer **3** and unstable dark pink rods of **1** (under reflux) or a mixture of **1** and **2** (solvothermal) was obtained. At pH above 3.5 and conducting the reaction under reflux or solvothermally yielded pink prisms of $[Co(C_2O_4)(NH_3)_4]_8[\beta\text{-}Mo_8O_{26}(H_2O)_2][\gamma\text{-}Mo_8O_{26}]\cdot 12H_2O$ (**4**) that were completely transformed into pink prisms of $[Co(C_2O_4)(NH_3)_4]_4[\gamma\text{-}Mo_8O_{26}(H_2O)_2]\cdot 6H_2O$ (**5**) within 24 hours. It seems that acetic acid as a poor chelating ligand allowed the formation of the corresponding discrete octamolybdates or an octamolybdate-based polymer, as the dominant species.

Most of the reactions carried out at higher temperatures and/or under higher pressure with the addition of succinic acid resulted in the formation of the β- and γ-octamolybdate mixture, or polymeric species $\{Mo_4O_{12}\}_n$, $\{Na_2Mo_8O_{29}(H_2O)_4\}_n$ and $\{\gamma\text{-}Mo_8O_{26}\}_n$ as the main products. Different reaction outcomes can be attributed to better chelating properties of succinic acid when compared to acetic acid.

Reactions carried out at higher temperatures (under reflux or solvothermally) in the presence of succinic acid (in the pH range 3.5 to 5.0) yielded initially a pink powder which upon standing under room temperature transformed into a mixture of oxomolybdates: hybrid octamolybdates **1** (unstable dark pink rods) and $[Co(C_2O_4)(NH_3)_4]_4[Mo_8O_{26}(H_2O)_2]\cdot 12H_2O$ (**7**) (light pink plates), octamolybdate-based cocrystal **6** (pink prisms), more complex polymer **3** (pink plates), and 2D metal–organic framework $[Co(C_2O_4)(NH_3)_4]_{2n}[Mo_4O_{12}(C_4H_4O_4)]_n\cdot 3nH_2O$ (**8**) (light pink needles). Reactions performed under reflux at pH value below 2.5 resulted in the formation of cocrystal **6**, while the solvothermally conducted reaction (pH around 2.0) additionally enabled isolation of a few red rods of polymer $[Co(C_2O_4)(NH_3)_4]_{4n}[\gamma\text{-}Mo_8O_{26}]_n\cdot 9nH_2O$ (**9**) before the formation of the final cocrystal **6**.

By applying the mechanochemical synthesis, all the reactions (independent of the type and the amount of carboxylic acid) yielded polymer **3** after the solid mixture, obtained by milling together sodium molybdate, tetraammineoxalatocobalt(III) nitrate and acid, was exposed to water vapor. Its exclusive formation can be attributed to the increased concentration of building units in the reaction mixture.

The isolation of polyoxomolybdates also depends on the properties of the applied counter ion, its electrostatic potential or its ability to stabilize the present polyoxo species through hydrogen bonding. This could be documented with results when performing the reactions with $[Co(CO_3)(NH_3)_4]^+$ (Table 1). A violet powder of $[Mo_5Co_2O_{17}(HCO_3)(C_4H_4O_4H)(NH_3)_7]\cdot 5H_2O$ (**10**) was observed as the only product of the reactions between tetraamminecarbonatocobalt(III) nitrate and sodium molybdate at pH below 4.0 (independent of the used synthetic approach and used carboxylic acid). If the violet powder was left to stand at room temperature in mother liquor for two months, its transformation resulted in $[Mo_5Co_2O_{18}(NH_3)_7]\cdot 5H_2O$ (**11**). The transformation of the amorphous precipitate of **10** to the crystalline product **11** is influenced by the stability of intermediates, $[Co(NH_3)_3]^{3+}$ and $[Co(NH_3)_4]^{3+}$ cations, formed in the reaction of $[Co(CO_3)(NH_3)_4]^+$ cations with carboxylic acids, as known from the

literature.[14] The same result was obtained at higher temperatures (solvothermal synthesis or under reflux) and lower pH values.

The presence of hydrogen succinate and hydrogen carbonate anions in **10** was corroborated by ^{13}C NMR and IR spectroscopy (Table S7, Fig. S9 and S10†). The ^{13}C NMR spectrum of **10** contained three signals at 35.92 ppm, 167.13 and 179.21 ppm arising from $C_4H_4O_4H^-$ and CO_3^{2-}/HCO_3^- anions. The signals observed at 35.92 and 179.21 belong to $H_4C_4O_4H^-$ while the signal at 167.13 to HCO_3^- anions, respectively. This is in accordance with the literature data.[22] Compound **11** was described in the literature but obtained by a different synthetic route.

Inspired by our previous investigation,[23] we aimed to explore the correlation of the hydrogen bonding ability of macrocations and the pH of the solution on the molybdovanadate formation. The solution-based synthesis of tetraammineoxalatocobalt(III) performed with the addition of ammonium vanadate led to the isolation of rose sticks of molybdovanadate $[Co(C_2O_4)(NH_3)_4]_2[H_2Mo_8V_5O_{40}Na_2(H_2O)_8]\cdot xH_2O$ (**12**) only when the reaction was conducted under reflux or solvothermally at pH value around 2.0. In all other solution-based reactions we were not able to isolate a product of defined composition. When $[Co(en)_3]^{3+}$ was used as a counterion, all the solution-based reactions resulted in the formation of a mixture of insoluble powder products. However, by applying a liquid-assisted ball milling method and exposing the solid mixture to water vapor we isolated yellow crystalline product $Na_3[Co(en)_3][HV_7Mo_2O_{27}]\cdot xH_2O$ (**13**).

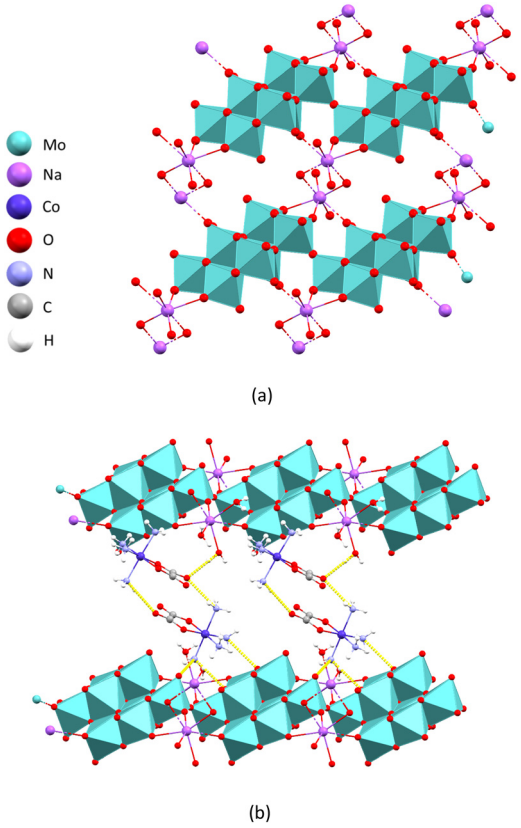

Fig. 1 Crystal structure of **3**: (a) a fragment of the two-dimensional coordination polymer layer perpendicular to the crystallographic *c* axis; and (b) crystal packing viewed along the crystallographic *b* axis of the coordination polymer layers (blue) bridged by hydrogen-bonded cobalt(III) cations and water molecules.

Structural studies

The oxomolybdates and molybdovanadates described in this paper were obtained through various reactions resulting in twelve crystalline compounds. Among these compounds, **1**, **2** and **11** have been previously described in the literature.[14] Compounds **3**–**9** are reported here for the first time (Table S9†). Compounds **12** and **13** were characterized in the solid state based on preliminary findings from single-crystal X-ray diffraction, along with data gathered from infrared spectroscopy and elemental analyses (see ESI†). Unfortunately, the crystals lacked the necessary quality for a satisfactory structural determination.

Polymer $[Co(C_2O_4)(NH_3)_4]_{4n}[Na_2Mo_8O_{29}(H_2O)_4]_n\cdot 6nH_2O$ (**3**) consists of octamolybdate chains interconnected by sodium cations. Each sodium cation is coordinated by seven oxygen atoms forming a distorted capped octahedron. Two vertices of the octahedron are occupied by oxygen atoms of the octamolybdate anion, with the remaining vertices being occupied by four water molecules, two of which are bridging water molecules between two sodium cations making the two oxygen polyhedra around sodium cations have (in **3** and **9**) a shared edge. An additional oxygen atom from the molybdate anion also coordinates the sodium cation with a longer bond length (d(Na1–O9) of 2.949(5) Å, as opposed to d(Na1–O4) of 2.325(4) Å or d(Na1–O5) of 2.632(5) Å) capping the octahedron on the face defined by the oxygen atom belonging to the first anion, a bridging water molecule and a terminal water molecule (Fig. 1a).

The structure of the polyoxomolybdate anion is in accordance with the ones previously reported.[24] There is an extensive network of hydrogen bonds between the coordination polymer layer, the ammine and oxalate ligands of the complex cation and water molecules interconnecting the former two. The ammine ligands of the cobalt(III) cation are oriented towards the negative oxygen atoms of the anion forming long hydrogen bonds (N4–H4B···O1^a of 2.953(5) Å, N4–H4C···O10^b of 3.033(6) Å, N4–H4A···O13^a of 3.029(6) Å, N7–H7A···O14^a of 2.992(5) Å and N8–H8A···O6^b of 3.042(5) Å; $a = -x, 1-y, 1-z$; $b = x, -1+y, z$).

The ammine groups and the oxalate groups of the cobalt(III) cations form a mutual hydrogen bond (N8–N8C···O17 of 2.976(6) Å), as well as hydrogen bonds with the surrounding water molecules, thus further interconnecting the layers into a three-dimensional supramolecular framework (Fig. 1b). The water molecules coordinated on the sodium atom also form hydrogen bonds with the oxygen atoms of the molybdate within the same layer (O3W–

H3WB···O12^{b} of 2.843(6) Å and O1W–H1WB···O7^{c} of 2.888(6) Å; $b = x, -1 + y, z$; $c = 1 + x, y, z$).

In the crystal lattice of $[Co(C_2O_4)(NH_3)_4]_8[\beta\text{-}Mo_8O_{26}(H_2O)_2][\gamma\text{-}Mo_8O_{26}(H_2O)_2]\cdot 12H_2O$ (**4**) are present two isomers of the octamolybdate anion: β-form and γ-form. This compound is the first example of a hybrid salt containing two isomers of the octamolybdate anion. The structure of both anions is consistent with similar structures described in the literature.[25] In compound **4**, anions and cations form a three-dimensional supramolecular network. The NH_3 molecules coordinated to the cobalt atom form hydrogen bonds with the oxalate ligands of neighboring cations, connecting cations in two-dimensional layers perpendicular to the crystallographic *a* axis (Fig. 2a). Layers of cations are bridged by anions forming hydrogen bonds with them (Fig. 2b). The β-octamolybdate anion forms eleven and γ-octamolybdate twelve bonds with $[Co(C_2O_4)(NH_3)_4]^+$ cations (Table S10†).

The water molecule coordinated to the molybdenum of the γ-octamolybdate anion forms an intramolecular hydrogen bond with the molybdate oxo ligand (O27–H27A···O19 of 3.197(12) Å) while the water molecules present in the crystal lattice also participate in the creation of an extensive supramolecular network.

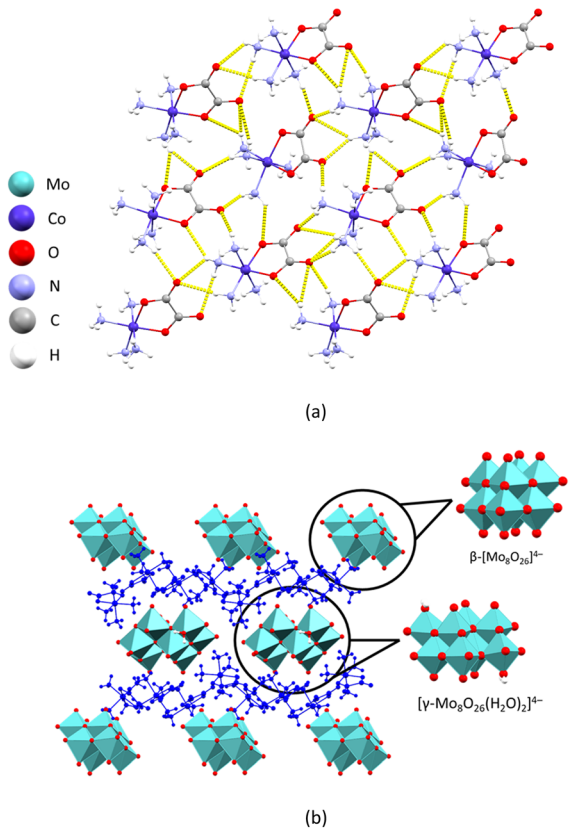

Fig. 2 Crystal structure of **4**: (a) supramolecular layer of hydrogen-bonded cations perpendicular to the crystallographic *c* axis; (b) unit cell packing viewed along the crystallographic *a* axis with layers of cations (blue) bridged by octamolybdate.

In compound $[Co(C_2O_4)(NH_3)_4]_4[\gamma\text{-}Mo_8O_{26}(H_2O)_2]\cdot 6H_2O$ (**5**), the γ-octamolybdate anion and four $[Co(C_2O_4)(NH_3)_4]^+$ cations crystallize as a hexahydrate salt. The crystal structure is an extensive three-dimensional supramolecular network of cations and anions connected by hydrogen bonds. The cations are connected by hydrogen bonds in a three-dimensional network, where the nitrogen atoms of the NH_3 group are donors of hydrogen bonds, and the oxygen atoms of oxalate ligands are acceptors. Water molecules also participate in the network. The structure built by complex cations contains voids in which octamolybdate anions are placed (Fig. 3). A water molecule coordinated to molybdenum of the γ-octamolybdate acts as a hydrogen bond donor and interacts with oxalate ligands (O14–H14B···O16^{a} of 3.049(6) Å and O14–H14B···O18^{a} of 2.800(6) Å; $a = 1 - x, 1 - y, 1 - z$), and the other oxygen atoms of molybdate anions are acceptors of hydrogen bonds that they create with NH_3 groups of cations.

The unit cell of $[Co(C_2O_4)(NH_3)_4]_4[\beta\text{-}Mo_8O_{26}]\cdot C_4H_6O_4\cdot 4H_2O$ (**6**) comprises four complex cobalt(III) cations, a β-octamolybdate anion, and a molecule of succinic acid. One of the two symmetrically independent complex cations (Co1) forms hydrogen bonds with succinic acid (N3–H3C···O22^{a} of 3.400(4) Å, N3–H3B···O23^{a} of 2.969(5) Å and O22–H22···O16^{b} of 2.830(4) Å; $a = 2 - x, 1 - y, 1 - z$; $b = x, y, z$) forming two-dimensional layers perpendicular to the crystallographic *b* axis (Fig. 4a). The layers are further interconnected by a series of hydrogen bonds (formed between the anions and the cations in the layers as well as the other symmetrically independent cation (Co2) and water molecules) resulting in an extensive three-dimensional supramolecular framework (Fig. 4b). Each anion participates in twenty-four hydrogen bonds with ammine ligands of the surrounding cations and water molecules, with the oxygen atoms of the molybdate anion acting as acceptors.

The structure of $[Co(C_2O_4)(NH_3)_4]_4[\gamma\text{-}Mo_8O_{26}(H_2O)_2]\cdot 12H_2O$ (**7**) contains a three-dimensional supramolecular framework consisting of γ-octamolybdate anions[26] hydrogen-bonded to $[Co(C_2O_4)(NH_3)_4]^+$ cations and water molecules. The NH_3 ligands of the cation form hydrogen bonds with oxygens from

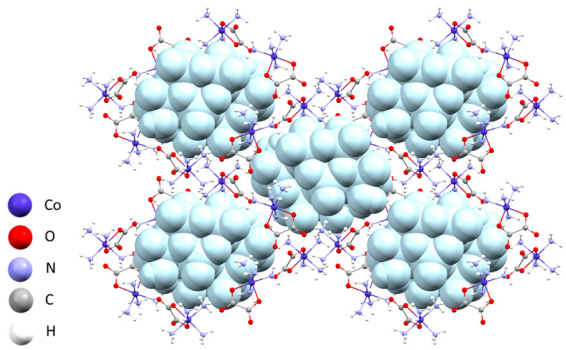

Fig. 3 Three-dimensional supramolecular network of $[Co(C_2O_4)(NH_3)_4]^+$ cations with molybdate anions (blue) located in voids in the crystal structure of compound **5**.

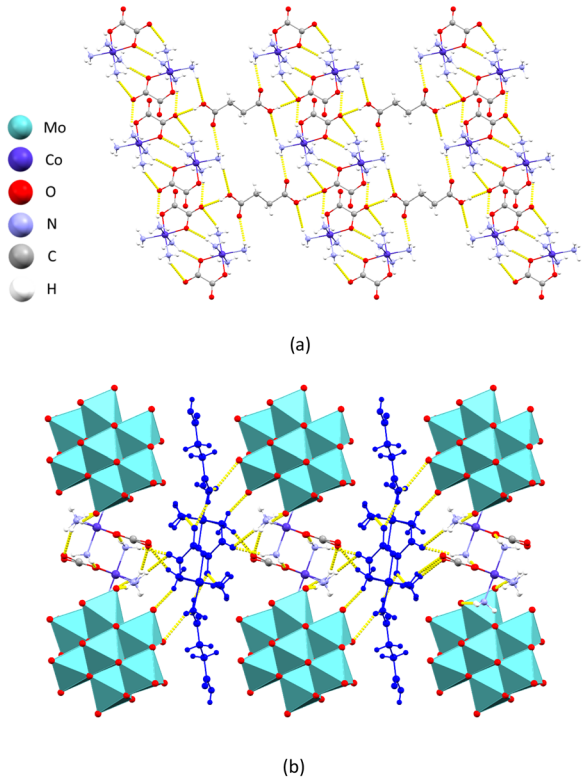

Fig. 4 Crystal structure of **6**: (a) fragment of the two-dimensional layer perpendicular to the crystallographic *b* axis comprising hydrogen-bonded cations bridged by succinic acid molecules; and (b) crystal packing viewed along the crystallographic *a* axis with layers of cations and succinic acid (gray) interconnected by molybdate anions and complex cobalt cations.

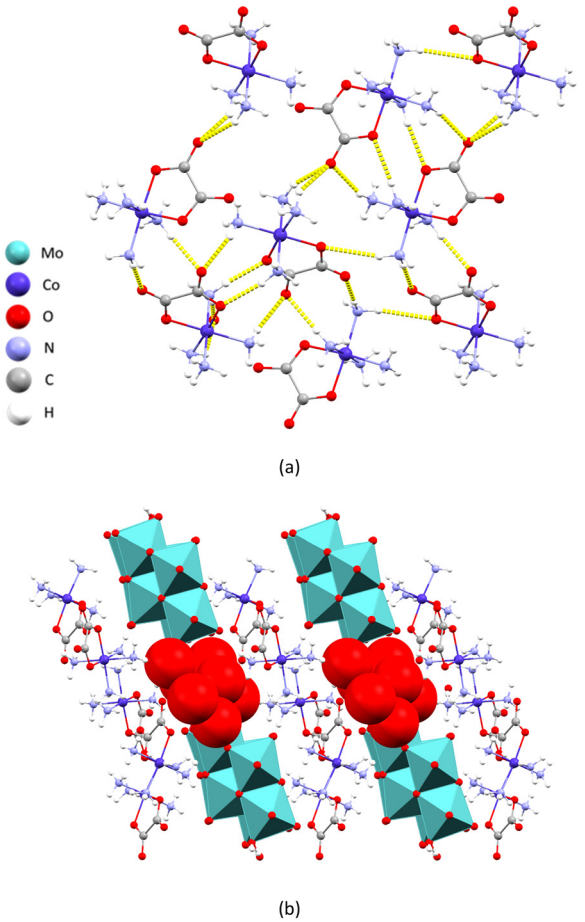

Fig. 5 Crystal structure of **7**: (a) fragment of the hydrogen-bonded two-dimensional cation layer perpendicular to the crystallographic *a* axis; and (b) crystal packing viewed along the crystallographic *c* axis with cations and anions forming channels containing water molecules.

oxalate ligands of other cations (N1–H1C···O22^{a} of 2.966(5) Å, N2–H2A···O21^{b} of 3.006(6) Å, N4–H4B···O18^{b} of 2.986(6) Å, N5–H5C···O20^{b} of 2.986(5) Å, N6–H6A···O22^{b} of 3.051(6) Å, N7–H7B···O18^{c} of 2.797(5) Å and N8–H8C···O18^{c} of 3.092(6) Å; $a = x, y, 1 + z$; $b = 2 - x, -y, 1 - z$; $c = x, y, z$) forming a two-dimensional layer perpendicular to the crystallographic *a* axis (Fig. 5a). The oxygen atoms of the molybdate anions act as acceptors of hydrogen bonds formed with the cation layers (N1–H1B···O11 of 2.946(6) Å, N2–H2B···O12 of 2.961(6) Å, N4–H4A···O1 of 3.088(6) Å and N5–H5A···O9 of 3.098(5) Å) expanding the layers into a 3D network.

The hydrogen-bonded network of anions and cations is arranged in a way that it leaves channels along the crystallographic *c* axis that contain water molecules (Fig. 5b). Additionally, two water molecules coordinated on molybdenum atoms also form hydrogen bonds with neighboring water molecules. This is the probable reason for a longer Mo1–O1W bond length (2.160(4) Å) compared to other terminal oxygen atoms with an average bond length of about 1.710 Å.

Compound $[Co(C_2O_4)(NH_3)_4]_{2n}[Mo_4O_{12}(C_4H_4O_4)]_n{\cdot}3nH_2O$ (**8**) is a two-dimensional metal–organic framework with polyoxomolybdate chains interconnected by coordinated succinate ions. The molybdate octahedra form a chain in a way that every octahedron shares an edge with two neighbouring ones making the three octahedra have a shared vertex. The succinate ions act as bridging ligands between four molybdenum ions, bidentate coordinating two neighbouring octahedra of the first chain and the two neighbouring octahedra of the second chain *via* two carboxyl groups (Fig. 6a). The geometry of the anion chain in **8** is similar to chains formed by MoO_6 octahedra in molybdenum(VI) oxide, the layers being separated by the succinate anions (Fig. 6b).[27]

The layers are interconnected by a series of hydrogen bonds formed between the oxygen atoms of the molybdate anions and the ammine ligands of the complex cobalt cation. Each monomeric unit of the anion participates in the formation of eleven N–H···O hydrogen bonds with the surrounding cations (Table S11†). The extensive network of hydrogen bonds connects the cations and anions into a three-dimensional supramolecular network with voids that contain additional water molecules (Fig. 6c).

The crystal structure of $[Co(C_2O_4)(NH_3)_4]_{4n}[\gamma\text{-}Mo_8O_{26}]_n{\cdot}9nH_2O$ (**9**) consists of complex cobalt(III) cations and infinite anionic molybdate chains built of

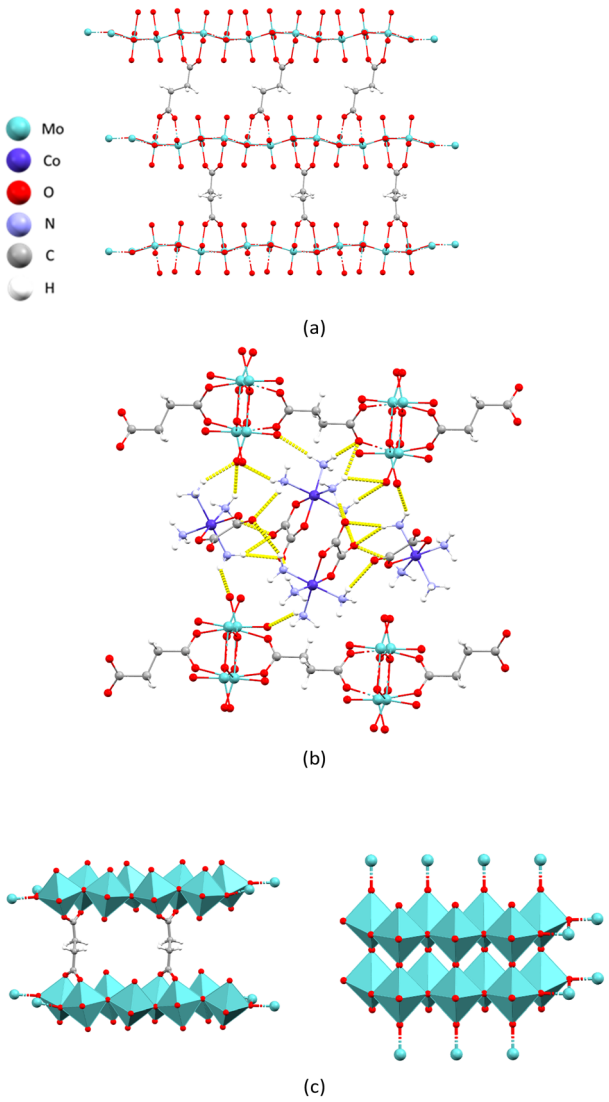

Fig. 6 Crystal structure of **8**: (a) fragment of the two-dimensional metal–organic framework layer perpendicular to the crystallographic *a* axis; (b) crystal packing viewed along the crystallographic *b* axis with a network of hydrogen-bonded cations and MOF layers; (c) polyhedral representation of the anionic chain in **8** (left) and layered structure of MoO_3 (right).

γ-octamolybdate units connected by a pair of shared vertices (Fig. 7a). The octamolybdate subunits found in **9** are isostructural with those found in the literature.[28] The polyanions are interconnected by a series of hydrogen bonds formed between oxygens of the anion and the hydrogens from the ammine ligands of the cations. Each $\{Mo_8O_{24}\}$ monomer participates in the formation of eleven hydrogen bonds with the surrounding cations (Table S12†). The cations are further connected through hydrogen-bonding of oxygen atoms of the oxalate ligands and the hydrogen atoms of the ammine ligands connecting the overall structure into a three-dimensional supramolecular network that leaves channels containing water molecules (Fig. 7).

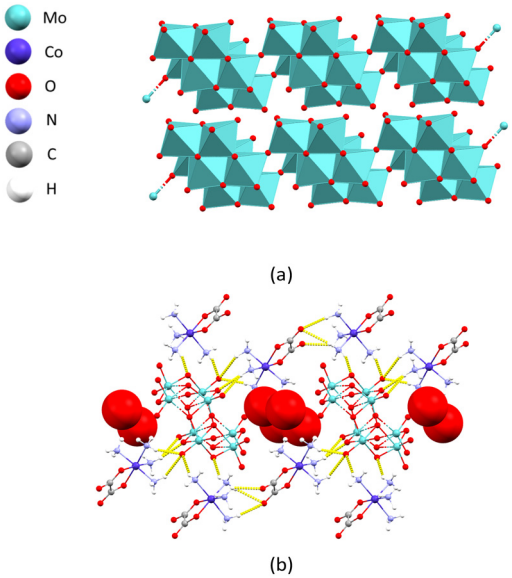

Fig. 7 Crystal structure of **9**: (a) polyhedral representation of polyanionic $[\gamma\text{-}Mo_8O_{26}]^{4-}$ chains; (b) crystal packing viewed along the crystallographic *a* axis showing a three-dimensional supramolecular network of hydrogen-bonded cations and anions with channels containing water molecules.

XPRD, spectroscopic and thermal investigations

To further study the purity of all crystals, the bulk products were crushed into a fine powder suitable for PXRD analysis. The PXRD patterns confirmed that the bulk powder is a single-phase material. As shown in Fig. 8 and Fig. S11–S14 (see ESI†), the diffraction peak positions in the experimental PXRD patterns for samples **1–9** agree well with the simulated patterns. This indicates that the structures of the bulk powders are consistent with those of single crystals, confirming that the phase purity is satisfactory.

The IR spectra of the prepared compounds **1–13** were examined in detail (Table S7†) and related to the structural information obtained by X-ray analysis and to the data reported in the literature.[29,30] In **1–10**, **12** and **13** the strong bands between 993 cm^{-1} and 822 cm^{-1} were assigned to the stretching vibrations of the terminal Mo–O bonds. The very strong bands observed in the regions between 836 and 796 cm^{-1} and 575 and 484 cm^{-1}, respectively, were assigned to

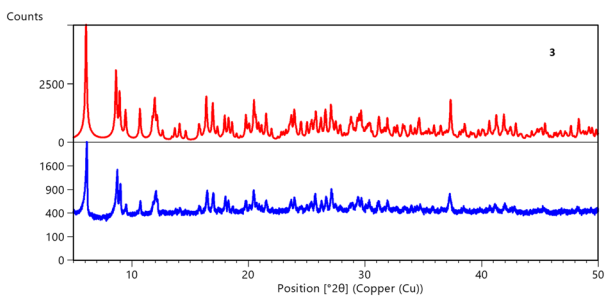

Fig. 8 PXRD patterns of compound **3**: red – simulated pattern; blue – experimental pattern.

Mo–O stretching within the Mo–O–Mo bridge. The broad and medium intensity bands present at 3498–3286 cm^{-1} confirmed the existence of the O–H···O hydrogen bonds. In the IR spectra of all the compounds, the strong bands at 1744–1699 cm^{-1} and 1560–1289 cm^{-1} were assigned to the asymmetric and symmetric stretching vibrations of C–O and C–C from the oxalate ligand present in the Co(III) complex cation and succinate ligand (present in **8** and **10**) or succinic acid (present in **6**).

Thermogravimetric studies were conducted on all products under an oxygen atmosphere and in the temperature interval of 25–600 °C (Fig. S1–S8,† Table S6). The dehydration and decomposition of the anhydrous part of the examined compounds were observed, and agreed with other investigations, *e.g.* structural analysis and literature data.[31] The decompositions of compounds **1–4**, **6**, **8**, and **10–12** proceeded in three steps, starting with the endothermic process associated with the loss of water molecules of crystallization (in the range of 36–146 °C for **1**; 46–155 °C for **2**; 37–166 °C for **3**; 126–296 °C for **4**; 36–103 °C for **6**; 33–291 °C for **7**; 39–100 °C for **8**; 28–155 °C for **10**; 31–154 °C for **11**; 40–282 °C for **12**).

For compound **4**, the initial step began at a notably higher temperature of 126 °C, unlike the other compounds examined. This observation can be attributed to the interactions between the two-dimensional layers, specifically to a series of hydrogen bonds involving water molecules, β- and γ-octamolybdate anions, and Co(III) cations. In contrast, compound **7** exhibits solvent loss at a significantly lower temperature of 33 °C. This can likely be attributed to the presence of water molecules within the channels of the structure, which are formed by the hydrogen bonding between the cations and γ-octamolybdate anions. The TG curves for compounds **4** and **7** are presented in Fig. 9. Additional data for compounds **1–3**, **5**, **6**, and **8–12** can be found in the ESI,† Fig. S1–S8.

The notable further weight loss can be attributed to the degradation of the unsolvated species in two distinct stages. The first one occurred in the temperature range of 146–316 °C (for **1**; 155–316 °C for **2**; 166–287 °C for **3**; 206–297 °C for **4**; 103–331 °C for **6**; 291–383 °C for **7**; 120–300 °C for **8**; 155–298 for **10**; 154–298 °C for **11**; 282–342 °C for **12**) and the second stage in the range of 316–361 °C (for **1**; 316–398 °C for **2**; 287–353 °C for **3**; 297–434 °C for **4**; 331–499 °C for **6**; 320–385 °C for **8**; 298–395 °C for **10**; 298–365 °C for **11**; 342–389 °C for **12**). These two stages represent the decomposition of Co-cation and oxomolybdate cores. The residual solids consisted of mixtures of $Co_xMo_yO_z$ (of **1**, **2**, **4**, **6**, **7**, **8**, **10**, and **11**) or $NaCo_xMo_yO_z$ (of **3**) or $Co_xMo_zV_y$ (of **12**).

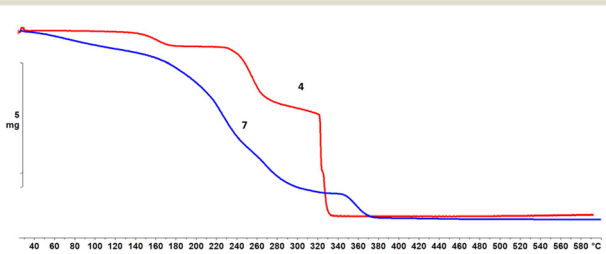

Fig. 9 The TG-curves for compounds **4** (red) and **7** (blue).

Conclusions

We synthesized and structurally characterized seven polyoxomolybdates and two molybdovanadates with varying nuclearities. These salts include $\{Na_2Mo_8O_{29}(H_2O)_4\}_n^{4m-}$, $\{[\beta\text{-}Mo_8O_{26}(H_2O)_2][\gamma\text{-}Mo_8O_{26}]\}^{8-}$, $\{\beta\text{-}Mo_8O_{26}(H_2O)_2\}^{4-}$, $\{Mo_4O_{12}(C_4H_4O_4)\}_n^{4m-}$, and $\{\gamma\text{-}Mo_8O_{26}\}_n^{4m-}$ anions, which represent to the best of our knowledge the first reported structures of that kind. The assembly processes are sensitive to the type of carboxylic acid used, and both succinic and acetic acids promote the formation of hybrid polyoxomolybdates. However, it is important to note that reaction temperature and pressure also play a significant role in influencing the polymerization process. Under reflux or hydrothermal conditions, octamolybdate[32] emerges as the primary structural framework in the products obtained. This is largely attributed to the thermal stability of the species involved in the equilibria present in aqueous solution. The less dense three-dimensional supramolecular framework, comprising either β- or γ-octamolybdates, is preferentially formed within the pH range between 2 and 5. In this pH range at room temperature, the dominant species consist of discrete $Mo_8O_{26}^{4-}$ units or the chains built up from $Mo_8O_{26}^{4-}$ connected with sodium cations. Lastly, we isolated the molybdovanadate $Na_3[Co(en)_3][HV_7Mo_2O_{27}]$ by exposing a solid reaction mixture to water vapor, which opens up new avenues for exploring the chemistry of molybdovanadates.

Experimental section

General methods and materials

Starting cobalt(III) complex salts, $[Co(CO_3)(NH_3)_4]NO_3{\cdot}H_2O$, $[Co(en)_3]Cl_3$ and $[Co(C_2O_4)(NH_3)_4]NO_3{\cdot}H_2O$ used as reaction precursors, were prepared according to the literature data.[33] $Na_2MoO_4{\cdot}2H_2O$, NH_4VO_3, acetic acid and succinic acid were commercially available reagent-grade chemicals that were employed as received without further purification. Elemental analyses were provided by the Analytical Services Laboratory of the Ruđer Bošković Institute, Zagreb and by the Analytical Services Laboratory of the Faculty of Science and Faculty of Forestry, University of Zagreb. Thermal studies (TGA-SDTA) were performed on a Mettler Toledo TGA/DSC3+ STARe Systems instrument using aluminum oxide crucibles under an O_2 atmosphere and in the temperature range from 25 to 600 °C. The heating rate was 10 °C min^{-1}. Infrared spectra were recorded on a PerkinElmer Spectrum RXI FTIR-ATR spectrometer in a 4000–400 cm^{-1} range. ^{13}C NMR spectra were recorded on a Bruker Avance III HD 400 spectrometer operating at 400 MHz. Compounds were dissolved in a mixture of NaOH and D_2O and measured in 5 mm NMR tubes at 298 K with TMS as the internal standard. The

sample concentration was 10 mg mL^{-1}. Single-crystal X-ray diffraction data of **1–9** and **11** were collected on an XtaLAB Synergy-*S* CCD diffractometer with CuK_α (λ = 154184 Å) radiation at room temperature or at 170 K. Data reduction was performed using the CrysAlis software package.[34] Solution, refinement and analysis of the structures were performed using the programs integrated in the WinGX[35] and OLEX2[36] systems. All structures were solved and refined with the SHELX program suite.[37] Structural refinement was performed on F^2 using all data. All hydrogen atoms were placed at calculated positions and treated as riding on their parent atoms. Geometrical calculations were performed using PLATON.[38] Drawings of the structures were prepared using PLATON and MERCURY programs.[39] Powder X-ray diffraction (PXRD) data were collected on a Malvern Panalytical Aeris powder diffractometer in the Bragg–Brentano geometry with a PIXcel^{1D} detector, using CuK_α radiation (λ = 1.5406 Å). Samples were contained on a Si sample holder. Powder patterns were collected at room temperature in the range from 5° to 50° (2θ) with a step size of 0.043° and 7.14 s per step. The data were collected and visualized by using the Malvern Panalytical HighScore Software Suite.[40]

Procedures for the synthesis of compounds 1–13. By solution based methods at room temperature (Method a), reflux (Method b), in an autoclave at 110 °C (Method c) and liquid-assisted ball milling followed by vapor-assisted aging (Method d) with $[Co(C_2O_4)(NH_3)_4]NO_3{\cdot}H_2O$, $[Co(CO_3)(NH_3)_4]NO_3{\cdot}H_2O$ or $[Co(en)_3]Cl_3$ as precursors. Experimental details, analytical and spectroscopic data are given in the ESI (Tables S1–S8†).

General procedure for solution-based methods. The aqueous solution (5 mL) containing sodium molybdate (5 mmol) and acetic or succinic acid, respectively, was added to an aqueous solution (15 mL) of the Co(III) complex salt (2 mmol). Depending on the amount of added acid, the pH value of the resulting reaction mixture was in the range between 2.0 and 5.0. The resulting reaction mixture was left to stand at room temperature for several days, or was refluxed for 2 hours, or heated for 1.5 hours in an autoclave at 110 °C, respectively.

All isolated products were filtered off, washed with cold water and dried to constant mass in a desiccator. In the case when the final product was a mixture of crystals, they were separated mechanically, washed with cold water and dried to constant mass in a desiccator.

Methods a) and c). When the complex salt $[Co(C_2O_4)(NH_3)_4]NO_3{\cdot}H_2O$ was used as a precursor, regardless of the amount of added acetic acid, the mixture of crystals of $[Co(C_2O_4)(NH_3)_4]_4[\beta\text{-}Mo_8O_{26}]{\cdot}12H_2O$ (**1**) and $[Co(C_2O_4)(NH_3)_4]_4[\beta\text{-}Mo_8O_{26}]{\cdot}10H_2O$ (**2**) was isolated (yield of **1**: 53 mg 36.30%; **2**: 46 mg 35.40%). At higher pH and by method c) crystals of $[Co(C_2O_4)(NH_3)_4]_4[\beta\text{-}Mo_8O_{26}(H_2O)_2][\gamma\text{-}Mo_8O_{26}]{\cdot}12H_2O$ (**4**) and $[Co(C_2O_4)(NH_3)_4]_4[\beta\text{-}Mo_8O_{26}(H_2O)_2]{\cdot}6H_2O$ (**5**) were isolated additionally (yield of **4**: 41 mg 34.30%; **5**: 1 mg). In the reaction with 1.22 mmol of succinic acid, the first product was a pink voluminous powder which was transformed to $[Co(C_2O_4)(NH_3)_4]_{4n}[Na_2Mo_8O_{29}(H_2O)_4]_n{\cdot}6nH_2O$ (**3**) (yield of **3**: 48 mg 40.38%). The transformation ended after three to four days. When a higher amount of succinic acid (2.44 mmol) was used, the first product was a pink voluminous powder which was transformed to **1** (yield of **1**: 51 mg 34.29%) within 24 hours or to $[Co(C_2O_4)(NH_3)_4]_4[Mo_8O_{26}]{\cdot}4H_2O{\cdot}C_4H_6O_4$ (**6**) (yield of **6**: 98 mg 82.50%) in the case when the reaction was carried out in an autoclave. The same product **6** was isolated at much higher concentrations of acid (7.93 or 15.90 mmol) regardless of the used synthetic method (yield of **6**: 96.07 mg 83.85% or 107.00 mg 93.45%). In the reaction carried out in an autoclave several pink rods of $[Co(C_2O_4)(NH_3)_4]_{4n}[\gamma\text{-}Mo_8O_{26}]_n{\cdot}9nH_2O$ (**9**) were also isolated (yield of **9**: 0.3 mg).

Method b). With the $[Co(C_2O_4)(NH_3)_4]NO_3{\cdot}H_2O$ complex salt as a precursor and by the addition of 1.22 or 2.44 mmol of acetic acid, crystals of **3** were isolated as the only reaction product (yield of **3**: 54.00 mg 45.43%). If the higher amounts of added acid mixture were used, a mixture of **1** and **3** and crystals of $[Co(C_2O_4)(NH_3)_4]_4[\beta\text{-}Mo_8O_{26}(H_2O)_2][\gamma\text{-}Mo_8O_{26}]{\cdot}12H_2O$ (**4**) and $[Co(C_2O_4)(NH_3)_4]_4[\beta\text{-}Mo_8O_{26}(H_2O)_2]{\cdot}6H_2O$ (**5**) were isolated (yield of **1**: 30.00 mg 36.29%; **3**: 25.34 mg 21.32%; **4**: 23.11 mg 17.57%; **5**: 2.5 mg). In reactions with succinic acid, depending on the amount of added acid crystalline product **3** (yield of **3**: 98 mg 82.49%) or a mixture of **1** (yield of **1**: 25.56 mg 22.07%), $[Co(C_2O_4)(NH_3)_4]_4[\gamma\text{-}Mo_8O_{26}(H_2O)_2]{\cdot}12H_2O$ (**7**) (yield of **7**: 41.00 mg 34.30%) and $[Co(C_2O_4)(NH_3)_4]_{2n}[Mo_4O_{12}(C_4H_4O_4)]_n{\cdot}3nH_2O$ (**8**) (yield of **8**: 12.00 mg 9.42%) was isolated.

Methods b) and c). With the $[Co(C_2O_4)(NH_3)_4]NO_3{\cdot}H_2O$ complex salt as a precursor and by the addition of NH_4VO_3 (5 mmol), acetic or succinic acid (1.22, 2.44, 7.53, 15.90 mmol), crystals of $[Co(C_2O_4)(NH_3)_4]_2[H_2Mo_8V_5O_{40}Na_2(H_2O)_8]{\cdot}xH_2O$ (**12**) (yield of **12**: 28.33 mg) were isolated as the main reaction product.

Methods a) and c). When the complex salt $[Co(CO_3)(NH_3)_4]NO_3$ was used as a precursor, regardless of the amount of added succinic acid, compounds $[Mo_5Co_2O_{17}(HCO_3)(H_4O_4C_4H)(NH_3)_7]{\cdot}5H_2O$ (**10**) (yield of **10**: 20.42 mg 17.93%) and $[Mo_5Co_2O_{18}(NH_3)_7]{\cdot}5H_2O$ (**11**) (yield of **11**: 62.09 mg 55.32%) were isolated at room temperature. Immediately after mixing the solutions (independent of the pH value) a violet voluminous powder of **10** was obtained. The same product was obtained in reactions carried out in an autoclave and with the addition of higher amounts of succinic acid. The product **10** was collected by filtration, washed with a small amount of cold water and dried to constant weight in a desiccator. When the violet powder was allowed to stand at room temperature in the mother liquor for one month, it was transformed into violet crystals **11**. Product **11** was collected by filtration, washed with a small amount of cold water and dried to constant weight in a desiccator (yield of **11**: 74.54 mg 66.07%).

Methods b) and c). With the $[Co(CO_3)(NH_3)_4]NO_3$ complex salt as a precursor, all the reactions conducted at room temperature (regardless of the pH value) resulted in the

formation of **10** and **11** (yield of **10**: 16.22 mg 14.30%; **11**: 54.11 mg 48.45%) respectively. We were able to isolate the above-mentioned products at higher-temperature only when the highest amounts of acid were used (pH 3–4). All the other reactions conducted at elevated temperature resulted in the formation of a green-brown solution and precipitation of an unidentified black-brown precipitate.

General procedure for liquid-assisted ball milling followed by vapour-assisted aging

a) $Na_2MoO_4{\cdot}2H_2O$ (5 mmol), Co(III) salt (2 mmol), acetic or succinic acid (1.22, 2.44, 7.53, 15.90 mmol) and acetone (25 μL) were placed within a 10 mL stainless steel jar. The reactants were milled for 1 hour at 25 Hz frequency. The produced pink solid reaction mixture was exposed to 100% humidity at room temperature. In all cases, the transformation resulted in the crystalline product **3** (yield of **3**: 14.00 mg 11.78% or 11.67 mg 9.82% or 14.89 mg 12.52%), regardless of the added acid or its amount.

b) $Na_2MoO_4{\cdot}2H_2O$ (5 mmol), NH_4VO_3 (5 mmol), Co(III) salt (2 mmol), acetic or succinic acid (1.22, 2.44, 7.53, 15.90 mmol) and acetone (25 μL) were placed in a 10 mL stainless steel jar. The reactants were milled for 1 hour at 25 Hz frequency. The produced rose solid reaction mixture was exposed to 100% humidity at room temperature. From all the solid reaction mixtures, after their exposure to water vapour, crystalline product **13** (yield of **13**: 4.21 mg) was obtained, regardless if the reaction was conducted with or without carboxylic acid.

For compounds **5**, **9** and **13** thermogravimetric analysis as well as elemental analysis for **5** and **9** could not be performed since only several crystals were produced. The obtained amount of these compounds was only sufficient for their single-crystal XRD analysis and IR spectroscopic characterization.

All products were filtered off, washed with cold water and dried to constant mass in a desiccator.

Data availability

The data supporting this article have been included as part of the ESI.† Crystallographic data for **3**–**9**, **12**, and **13** have been deposited at the Cambridge Structural Database under deposition numbers CCDC 2404581–2404589.

Author contributions

Conceptualization, M. C.; investigation, M. C., D. K., V. D.; writing—original draft preparation, M. C., D. K.; project administration, V. V.; funding acquisition, V. V.; review and editing, V. V. All authors have read and agreed to the published version of the manuscript.

Conflicts of interest

There are no conflicts to declare.

Acknowledgements

This work was supported by the Croatian Science Foundation under the project number HRZZ-IP-2022-10-7368. We acknowledge the support of project CIuK co-financed by the Croatian Government and the European Union through the European Regional Development Fund—Competitiveness and Cohesion Operational Programme (Grant KK.01.1.1.02.0016).

Notes and references

1 (*a*) X. L. Wang, C. Qin, E. B. Wang, Z. M. Su, Y. G. Li and L. Xu, *Angew. Chem., Int. Ed.*, 2006, **45**, 7411; (*b*) M. T. Pope and A. Müller, *Angew. Chem., Int. Ed. Engl.*, 1991, **103**, 56.
2 D. L. Long, E. Burkholder and L. Cronin, *Chem. Soc. Rev.*, 2007, **36**, 105.
3 (*a*) D. L. Long, R. Tsunashima and L. Cronin, *Angew. Chem., Int. Ed.*, 2010, **49**, 1736; (*b*) N. Mizuno and M. Misono, *Chem. Rev.*, 1998, **98**, 199; (*c*) Q. S. Yin, J. M. Tan, C. Besson, Y. V. Geletii, D. G. Musaev, A. E. Kuznetsov, Z. Luo, K. I. Hardcastle and C. L. Hill, *Science*, 2010, **328**, 342.
4 J. J. Cruywagen, A. G. Draaijer, J. B. B. Heyns and E. A. Rogwer, *Inorg. Chim. Acta*, 2002, **331**, 322.
5 J. Pisk, V. Vrdoljak, M. Mandarić, T. Hrenar, D. Agustin and M. Rubčić, *RSC Adv.*, 2024, **14**, 19029.
6 N. Bebić, E. Topić, M. Mandarić, T. Hrenar and V. Vrdoljak, *CrystEngComm*, 2021, **23**, 6349.
7 A. Misra, K. Kozma, C. Streb and M. Nyman, *Angew. Chem.*, 2020, **59**(2), 596.
8 (*a*) V. W. Day, M. F. Fredrich, W. G. Klemperer and W. Shum, *J. Am. Chem. Soc.*, 1977, **99**, 6146; (*b*) T. C. Hsieh, S. N. Shaikh and J. Zubieta, *Inorg. Chem.*, 1987, **26**(24), 4079; (*c*) B. Kamenar, B. Korpar-Čolig, M. Penavić and M. Cindrić, *J. Chem. Soc., Dalton Trans.*, 1990, 1125; (*d*) M. L. Niven, J. J. Cruywagen and J. B. B. Heyns, *J. Chem. Soc., Dalton Trans.*, 1991, 2007; (*e*) M. Inoue and T. Yamase, *Bull. Chem. Soc. Jpn.*, 1995, **68**, 3055.
9 (*a*) T. J. R. Weakley, *Polyhedron*, 1982, **1**(1), 17; (*b*) I. Zebiri, S. Boufas, S. Mosbah, L. Bencharif and M. Bencharif, *J. Chem. Sci.*, 2015, **127**(10), 1769; (*c*) R. Z. Wang, J. Q. Xu, G. Y. Yang, W. M. Bu, Y. H. Xing, D. M. Li, S. Q. Liu, L. Ye and Y. G. Fan, *Polyhedron*, 1999, **18**, 2971; (*d*) R. Z. Wang, J. Q. Xu, G. Y. Yang, Y. F. Li, Y. H. Xing, D. M. Li, S. Q. Liu, L. W. M. Bu, L. Ye and Y. G. Fan, *Solid State Sci.*, 2000, **2**, 705.
10 (*a*) D. Hagrman, C. Zubieta, D. J. Pink, J. Zubieta and R. C. Haushalter, *Angew. Chem., Int. Ed. Engl.*, 1997, **36**, 873; (*b*) J. Q. Xu, R. Z. Wang, G. Y. Yang, Y. H. Xing, D. M. Li, W. M. Bu, L. Ye, Y. G. Fan, G. D. Yang, Y. Xing, Y. H. Lin and H. Q. Jia, *Chem. Commun.*, 1999, 983.
11 A. J. Bridgeman, *J. Phys. Chem. A*, 2002, **106**, 12151.
12 M. T. Pope and A. Müller, *Polyoxometalate Chemistry From Topology via Self-Assembly to Applications*, Kluwer, Dordrecht, 2001, p. 269.
13 R. Xi, B. Wang, K. Isobe, T. Nishioka, K. Toriumi and Y. Ozawa, *Inorg. Chem.*, 1994, **33**, 833.

14 J. Fuchs and H. Hartl, *Angew. Chem., Int. Ed. Engl.*, 1976, **15**, 375.
15 L. Atovmyan and O. Krasochka, *Struct. Chem.*, 1972, **13**, 319.
16 A. Szymańska, W. Nitek, D. Rutkowska-Zbik and W. Łasocha, *Monatsh. Chem.*, 2014, **145**(6), 921.
17 P. J. Hagrman, D. Hagrman and J. Zubieta, *Angew. Chem., Int. Ed.*, 1999, **38**(18), 2638.
18 D. Kuzman, V. Damjanović, V. Stilinović, M. Cindrić and V. Vrdoljak, *New J. Chem.*, 2021, **45**, 19764.
19 V. Damjanović, D. Kuzman, V. Vrdoljak, S. Muratović, D. Žilić, V. Stilinović and M. Cindrić, *Cryst. Growth Des.*, 2019, **19**, 6763.
20 D. Kuzman, V. Damjanović, V. Vrdoljak, V. Stilinović and M. Cindrić, *Inorg. Chim. Acta*, 2020, **510**, 119765.
21 N. I. Gumerova and A. Rompel, *Chem. Soc. Rev.*, 2020, **49**, 7568.
22 S. Morete, P. J. Dyson and G. Laurenczy, *Dalton Trans.*, 2013, **42**, 4353.
23 V. Damjanović, J. Pisk, D. Kuzman, D. Agustin, V. Vrdoljak, V. Stilinović and M. Cindrić, *Dalton Trans.*, 2019, **48**, 9974.
24 (*a*) I. Böschen, B. Buss and B. Krebs, *Acta Crystallogr., Sect. B: Struct. Sci., Cryst. Eng. Mater.*, 1974, **30**, 48; (*b*) T. Yamase and H. Naruke, *J. Chem. Soc., Dalton Trans.*, 1991, 285; (*c*) T. Yamase, T. Ozeki and I. Kawashima, *Acta Crystallogr., Sect. C: Struct. Chem.*, 1995, **51**, 545; (*d*) A. S. Sukhikh, P. Khranenko, T. V. Basova and S. A. Gromilov, *J. Struct. Chem.*, 2022, **63**, 310.
25 (*a*) A. Kitamura, T. Ozeki and A. Yagasaki, *Inorg. Chem.*, 1997, **36**, 4275; (*b*) T. J. R. Weakley, *Polyhedron*, 1982, **1**, 17; (*c*) A. B. Kama, R. Dessapt, H. Serier-Brault, M. Sidibe, D. Cheikh, A. K. Diop and R. Gautier, *J. Mol. Struct.*, 2017, **1141**, 698; (*d*) X. Wang, D. Liu, H. Lin, G. Liu, X. Wang, M. Le and X. Rong, *CrystEngComm*, 2016, **18**, 888; (*e*) M. H. Rosnes, C. Y. D.-L. Long and L. Cronin, *Dalton Trans.*, 2012, **41**, 10071.
26 (*a*) E. Cartuyvels, K. Van Hecke, L. Van Meervelt, C. Gröller-Walrand and T. N. Parac-Vogt, *J. Inorg. Biochem.*, 2008, **102**, 1589; (*b*) M. Inoue and T. Yamase, *Bull. Chem. Soc. Jpn.*, 1995, **68**, 3055; (*c*) M. Tahmasebi, M. Mirzaei, H. Eshtiagh-Hosseini, J. T. Mague, A. Bauzá and A. Frontera, *Acta Crystallogr., Sect. C:Struct. Chem.*, 2019, **75**, 469; (*d*) R. Atencio, A. Briceño, P. Silva, J. A. Rodríguez and J. C. Hanson, *New J. Chem.*, 2007, **31**, 33; (*e*) E. M. McCarron III and R. L. Harlow, *J. Am. Chem. Soc.*, 1983, **105**, 6179; (*f*) T. Ito, K. Mikurube, K. Hasegawa, T. Matsumoto, K. Kosaka, H. Naruke and A. Koguchi, *Crystals*, 2014, **4**, 42; (*g*) B. Kamenar, M. Penavić and B. Marković, *Acta Crystallogr., Sect. C:Struct. Chem.*, 1988, **44**, 1521.
27 N. Wooster, *Z. Kristallogr. – Cryst. Mater.*, 1931, **80**, 504.
28 (*a*) Q.-G. Zhai, X.-Y. Wu, S.-M. Chen, Z.-G. Zhao and C.-Z. Lu, *Inorg. Chem.*, 2007, **46**, 5046; (*b*) X. Wang, J. Sun, H. Lin, Z. Chemng, X. Wang and G. Liu, *Dalton Trans.*, 2016, **45**, 12465; (*c*) H.-J. Du, Z.-Z. Shu, Y.-Y. Niu, L.-S. Song and Y. Zhu, *J. Solid State Chem.*, 2012, **190**, 296; (*d*) H. S. Casalongue, S. J. Choyke, A. N. Sarjeant, J. Schrier and A. J. Norquist, *J. Solid State Chem.*, 2009, **182**, 1297; (*e*) K. J. Thorn, A. N. Sarjeant and A. J. Norquist, *Acta Crystallogr., Sect. E: Crystallogr. Commun.*, 2005, **61**, m1665; (*f*) M. Evain, V. Petricek, V. Coué, R. Dessapt, M. Bujoli-Doeuff and S. Jobic, *Acta Crystallogr.*, 2006, **62**, 790.
29 M. Cindrić, V. Stilinović, M. Rubčić, G. Medak, D. Šišak Jung and V. Vrdoljak, *CrystEngComm*, 2018, **20**, 1889.
30 (*a*) Y. Chen, X. Shen, H. Zhang, C. Huang, Y. Cao and R. Sun, *Vib. Spectrosc.*, 2006, **40**, 142; (*b*) G. Mahata and K. Biradha, *Inorganica Chim. Acta*, 2007, **360**, 281; (*c*) E. McCarron, J. F. Whitney and D. B. Chase, *Inorg. Chim. Acta*, 1984, **23**, 3275; (*d*) R. P. Sharma, R. Bala, R. Sharma and P. Venugopalan, *J. Coord. Chem.*, 2004, **57**, 1563; (*e*) S. Ikegami and A. Yagasaki, *Materials*, 2009, **2**, 869.
31 P. Roman, A. Lique, J. M. Gutiérrez-Zorrilla and S. Garcia-Granada, *Polyhedron*, 1991, **10**, 2057.
32 J. Noack, F. Rosowski, R. Schlögl and A. Trunschke, *Z. Anorg. Allg. Chem.*, 2014, **640**(14), 2730.
33 (*a*) N. Hur, W. G. Klemperer and R. C. Wang, *Inorganic Synthesis*, John Wiley & Sons, New York, 1990, vol. 27, p. 77; (*b*) M. Mori, M. Shibata, E. Kyuno and E. Hoshiyama, *Bull. Chem. Soc. Jpn.*, 1958, **31**, 291; (*c*) P. C. Junk and J. W. Steed, *Polyhedron*, 1999, **18**, 3593; (*d*) R. A. Krause and E. A. Megargle, *J. Chem. Educ.*, 1976, **53**(10), 667.
34 Agilent, *CrysAlis PRO*, Agilent Technologies Ltd., Yarnton, Oxfordshire, England, 2014; *Oxford Diffraction, Xcalibur CCD system, CrysAlis CCD and CrysAlis RED software, Version 1.170*, Oxford Diffraction Ltd., 2003.
35 L. J. Farrugia, *J. Appl. Crystallogr.*, 2012, **45**, 849.
36 O. V. Dolomanov, L. J. Bourhis, R. J. Gildea, J. A. K. Howard and H. Puschmann, *J. Appl. Crystallogr.*, 2009, **42**, 339.
37 G. M. Sheldrick, *Acta Crystallogr., Sect. A*, 2015, **71**, 3.
38 A. L. Spek, *Acta Crystallogr., Sect. D:Biol. Crystallogr.*, 2009, **65**, 148.
39 C. F. Macrae, P. R. Edgington, P. McCabe, E. Pidcock, G. P. Shields, R. Taylor, M. Towler and J. van de Streek, *J. Appl. Crystallogr.*, 2006, **39**, 453.
40 T. Degen, M. Sadki, E. Bron, U. König and G. Nénert, *Powder Diffr.*, 2014, **29**(S2), S13.

